Journal of Statistics & Management Systems
ISSN 0972-0510 (Print), ISSN 2169-0014 (Online)
Vol. 29 (2026), No. 3, pp. 301–329
DOI : 10.47974/JSMS-1493

A characterizable probability model : Properties and flood data application

Fatimah E. Almuhayfith [§]
Department of Mathematics and Statistics
College of Science
King Faisal University
Alahsa 31982
Saudi Arabia

Tassaddaq Hussain [†]
Department of Mathematics
Mirpur University of Science and Technology (MUST)
Mirpur 10250
Pakistan

Hassan S. Bakouch *
Department of Mathematics
College of Science
Qassim University
Buraydah 51452
Saudi Arabia

and

Department of Mathematics
Faculty of Science
Tanta University
Tanta 31111
Egypt

[§] *E-mail:* **falmuhaifeez@kfu.edu.sa**
[†] *E-mail:* **tassaddaq.stat@must.edu.pk**
* *E-mail:* **h.bakouch@qu.edu.sa (Corresponding Author)**

Hanan H. El-Damrawy [‡]
Department of Mathematics
Faculty of Science
Tanta University
Tanta 31111
Egypt

Sadiah M. A. Aljeddani [@]
Department of Mathematics
Al-Lith University College
Umm Al-Qura University
Al-Lith 21961
Saudi Arabia

Abstract

As flood frequency analysis (FFA) is an exact and vigorous zone of analysis in statistical hydrology, so, in this regard, numerous probability models, parameters estimation procedures, regionalization problems, and other associated issues are being scrutinized in statistical hydrology. For this reason, research on FFA has been conducted with fluctuating passion over the past couple of decades. Therefore, there is a need to introduce flexible probability models and their parametric estimation techniques in statistical hydrology. However, for accurate probability modeling of upcoming flood events researchers try their best to study the heavy tailed distributions. In light of this, we intend to put forth a flexible probability model that not only addresses the problems with regional flood statistics but also illustrates the reasonable return periods for flood events brought on by melting glaciers and rising temperatures. We have described and examined some mathematical and statistical aspects of the suggested approach in light of the aforementioned scenario, and we have used it on actual flood data sets. To ensure realistic predictions using the proposed model, we have also analyzed it in terms of Mellin transformation.

Subject Classification (2010): *60E05, 62E15.*

Keywords: *Climate change, Hazard rate function, Link function, Goodness-of-fit statistics, Prediction, Data analysis.*

1. Introduction

Among all natural hazards, flooding ranks as one of the most severe and widespread globally. As a result, it impacts the country's economy, see Kumar et al. [10]. So, precise hazard impost is desirable to diminish flood loss. In this regard, the best tool for planning flood approximations is FFA. For this purpose, researchers typically take into account extreme value distributions. Flood

[‡] *E-mail:* **hanan.eldamarawi@science.tanta.edu.eg**
[@] *E-mail:* **smgadany@uqu.edu.sa**

Frequency Analysis (FFA) traditionally employs the Annual Maximum Flood (AMF) model, which constructs the AMF series by selecting the single highest flow value from each year's streamflow record. This approach remains the most commonly applied and globally accepted method in hydrological studies.

Nevertheless, alternative techniques have gained attention in recent years. These include: i) the Peaks-Over-Threshold (POT) method, which involves selecting flood events that exceed a variable threshold, thereby allowing for multiple events per year depending on the threshold setting; and ii) Regional Flood Frequency Analysis (RFFA), which aims to estimate flood quantiles for ungauged catchments by leveraging data from hydrologically similar regions.

Despite their potential advantages, both methods present notable challenges. The POT method may introduce dependencies among observations and is highly sensitive to threshold selection-lower thresholds can reduce bias but increase variance in large samples, with the inverse effect in smaller datasets (see Bommier [2]). RFFA, while promising, has seen limited application beyond specific regions or climatic zones (see Smith, Sampson, and Bates [20]). Furthermore, both methods involve more complex methodologies compared to the conventional AMF-based FFA.

It is therefore not possible to present appropriate probability models for the prediction of a realistic return period by using the distribution of the two approaches mentioned above due to their complexity.

FFA assists the researchers in choosing an appropriate probability model because a realistic return period is essential for policy-making to prevent future flood devastation as precisely as feasible. In view of this, we present a flexible stochastic model that will work equally well in all of discussed methods, like POT and RFFA, for the analysis of flood data. Flooding has a serious negative impact on all aspects of life, so in order to protect people, animals, and the environment, potential risks must be considered from the perspectives of readiness and anticipation. However, proactive measures are also necessary to avert disastrous outcomes in the event of a predicted threat, as highlighted by Neufeldt, Christiansen, and Dale [15] and Zakaria, Suleiman, and Mohamad [24].

The rapid changes in the world's climate are worrisome, as they are causing significant impacts on both the environment and human society. These effects include the spread of diseases, higher mortality rates, damage to infrastructure, and extreme weather events such as intense rainfall, storms, heatwaves, floods, and droughts. For a realistic assessment, FFA involves the following steps to accurately assess return periods: (i) data screening; (ii) selecting an appropriate distribution; and (iii) Determining the appropriate parameter estimation technique to fit the selected distribution to the available flood data. For this purpose, readers are referred to Hosking and Wallis [9], Hamed and Rao [7], Nouri Gheidari [16], Deng [4], Sagrillo, Guerra, and Bayer [19] and Hasan [8] for a thorough examination of the algorithms and execution of these specified stages.

However, the actual probability distribution of floods at a specific location or region is usually unknown, and it serves as the foundation for the entire FFA. To that end, the required probability distribution is usually selected from the existing classical distributions, which include the following: exponential distribution (ED), extreme value-I, -II and -III(Fréchet or EV-I, EV-II and EV-III), Pearson type III(P-III), gamma distribution(GD), three-parameter Kappa (KP3), Weibull (WD), Dagum (DD), Gumbel (GuD), logistic (LD), log-logistic (LLD), log-Pearson III (LP-III), and lognormal (LND), distributions, see Boorman [1], Millington, Das, and Simonovic [13], McCuen [14] and Cunnane [3].

Although some of them are regarded as national model for flood estimation in a nation, such as the GEV distribution recommended by Boorman [1], the LP-III distribution approved by the Institution of Engineers of Australia for flood frequency analysis, the P-III distribution endorsed by California, the LN-II distribution recommended by Italian flood data analysis, the LN-II distribution established by Canadian flood data analysis as the most appropriate, and U.S. Water Resources Council acknowledges the group's support for utilizing the LP-III distribution. However, the probability models like EV-I, EV-II, EV-III, GEV, LN, P3, GD(II, III), LP3 and ED are being used to model the flood frequency analyses around the world in 16, 9, 8, 2, 16, 12, 6, 13 and 4 countries, respectively, see Cunnane [3] and Webster and Stedinger [23]. In actuality, the aforementioned typical models are unsuitable for a realistic return period estimation since, even in the event that such evidence were available, a significant number of indefinite parameters would need to be evaluated, rendering the model useless for real-world applications, see Rowinski, Strupczewski, and Singh [17].

As the aggregate amount of high flood outflow is projected to rise around the globe during the current decade, so we are going to derive and propose a flexible probability model to address the situations like: i) realistic interpretation of the return period ii) predicting the floods occurrences, iii) capable of handling both stationarity and non-stationarity conditions. In this context, the derivation of the presented model, known as the power reciprocal distribution, will be discussed in the upcoming section.

The structure of the article is as follows: Section 2 focuses on the research methodology. Section 3 investigates the properties of the probability density function (PDF) and hazard rate function (HRF), along with the asymptotic structure of the proposed model. The quantile function and its characterization through the HRF are also explored. Section 4 presents further moments via Laplace and Mellin transforms, as well as the characterization through the Mellin transformation. Section 5 presents the order statistics with their asymptotic form. In Section 6, we examine the estimation of the model parameters using two approaches. Section 7 applies the proposed model to several flood datasets, while Section 8 offers concluding remarks on the paper.

2. Research Methodology

This section will describe the research methodology, and the following section will explore the key properties of the proposed distribution. The derivation approach for the proposed model is based on the steps outlined below.

- The most important step in this approach is to choose an odd link function $Q(.)$ that approaches (a, b) as $x \to 0$ and $x \to \infty$, respectively, and is both differentiable and monotonically non-decreasing.

- Odd link function is the ratio of cumulative distribution function (CDF) to the survival function (SF), and it is an important transformation for the T-X family of continuous distributions. A detailed review of this concept can be found in Khadim et al. [11] and Rehman et al. [22].
- Mathematically, it is formulated as: $\mathcal{Q}(x;\Theta) = \frac{\mathcal{G}(x;\Theta)}{1-\mathcal{G}(x;\Theta)}$ where, $\mathcal{G}(x;\Theta)$ is a baseline CDF and Θ contains a set of parameters.
- Assume a log-logistic distribution with parameters $(\theta = 1, \alpha)$, where the CDF serving as the baseline is given by $\mathrm{G}(x|\alpha, 1) = \frac{x}{x+\alpha}$, where $0 \leq x \leq \infty$.
- Incorporate the $\mathrm{G}(x|\alpha, 1)$ into the above link function $\mathcal{Q}(x|\alpha,\theta)$, so we get $\mathcal{Q}(x|\alpha,\theta) = \frac{\alpha}{x}$.
- After extracting the Fréchet CDF effect as $e^{-(\frac{\alpha}{x})^{\theta}} = \int_0^{\frac{\alpha}{x}} \theta e^{-t^{-\theta}} t^{-\theta-1} dt$ with SF $1 - e^{-(\frac{\alpha}{x})^{\theta}}$, where $f(t) = \theta e^{-t^{-\theta}} t^{-\theta-1}, 0 < t < \infty$ is the PDF of Fréchet distribution.
- In order to conclude the derivation, we consider a parallel series with a β number of components, the resulting survival expression can be written as $(1 - e^{-(\frac{\alpha}{x})^{\theta}})^{\beta}$.
- Therefore, the CDF of the proposed power reciprocal distribution (PRD) is formulated as

$$\mathcal{F}(x) = 1 - (1 - e^{-(\frac{\alpha}{x})^{\theta}})^{\beta}, x > 0, \theta, \beta, \alpha > 0. \tag{1}$$

Note that Equation (1) defines a valid CDF, because it satisfies all the required properties: $\mathcal{F}(0) = 0$ and $\mathcal{F}(\infty) = 1$.

Now, the definition of the proposed model can be stated as follows.

Definition 2.1: Let X follow $PRD(\alpha,\ \beta,\ \theta)$ with the CDF defined in Equation (1). By differentiating it with respect to x, we obtain the PDF of the proposed model, which is expressed as

$$f_{\mathrm{PRD}}(x;\alpha,\beta,\theta) = \frac{\theta\alpha\beta}{x^2\left(1-e^{-(\frac{\alpha}{x})^{\theta}}\right)^{1-\beta}} \left(\frac{\alpha}{x}\right)^{\theta-1} e^{-(\frac{\alpha}{x})^{\theta}}. \tag{2}$$

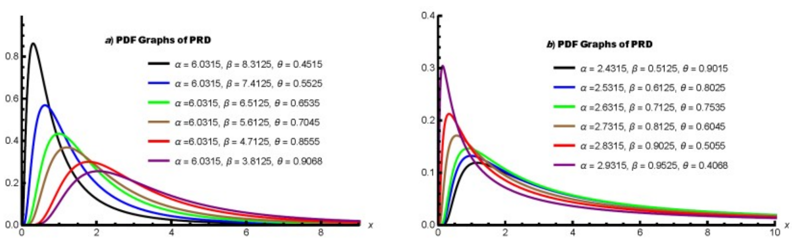

Figure 1
PDF graphs of PRD

The proposed model generates a positively skewed curve for $\alpha < 1$. The curve behaves like a leptokurtic, while for $\alpha > 1$ the curves portray platykurtic behavior (See Figure 1).

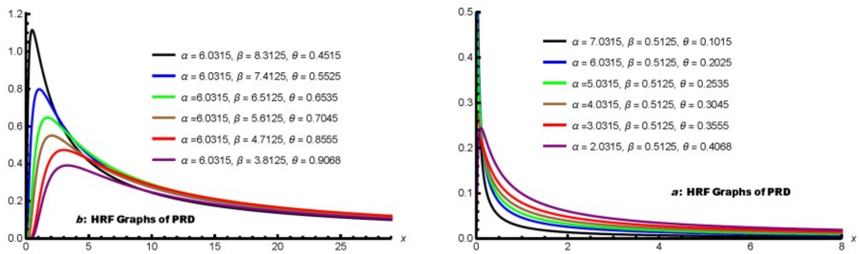

Figure 2
HRF graphs of PRD.

3. Results, including Statistical Properties of Proposed Model

This section is dedicated to investigating the statistical properties of the proposed model, including the curve behavior, HRF, and the functions of the PRD distribution. Additionally, we provide a characterization based on the HRF, which can be expressed in terms of the PDF and CDF for the random variable X as $\mathcal{H}(x) = \frac{f(x)}{\mathcal{S}(x)}$. The HRF can be defined as:

$$\mathcal{H}_{PRD}(x) = \frac{\theta\alpha\beta(\frac{\alpha}{x})^{\theta-1}e^{-(\frac{\alpha}{x})^{\theta}}}{x^2\left(1-e^{-(\frac{\alpha}{x})^{\theta}}\right).} \tag{3}$$

3.1 *Mode of the PRD*

To explore the curve behavior and modes of the PDF, we first express the logarithmic form of Equation (2). By differentiating this logarithmic form with respect to (w.r.t.) x and setting the derivative equal to zero, i.e., $(ln(f_{PRD}(x)))' = \frac{d}{dx}(ln(f_{PRD}(x))) = 0$, we obtain the following:

$$(ln(f_{PRD}(x)))' = \frac{\alpha\left(\frac{\alpha}{x}\right)^{-1+\theta}\theta}{x^2} - \frac{e^{-\left(\frac{\alpha}{x}\right)^{\theta}}\alpha\left(\frac{\alpha}{x}\right)^{-1+\theta}(-1+\beta)\theta}{\left(1-e^{-\left(\frac{\alpha}{x}\right)^{\theta}}\right)x^2} - \frac{\theta+1}{x} = 0. \tag{4}$$

Based on Equation 4, it is impossible to get a closed solution so we have to depend on a computational package, such as Mathematica [11.0] for its numerical optimization. We also observed for $x \to 0$, the $(\ln(f_{PRD}(0)))' = \infty$; for $x \to \infty$, the $(\ln(f_{PRD}(\infty)))' = 0$, and thus showing a non-monotonically decreasing behavior.

3.2 Hazard Rate Function and its Mode

The HRF of the PRD depicts increasing, decreasing and upside-down bathtub shape, so for $\alpha < 1$ the curve behaves like a bathtub, while for $\alpha > 1$

the curves increase and when $\theta < 1, \alpha > 1$, the HRF decreases, see Figure 2. However, when focusing on the risk in the immediate future, assuming the product has not failed by time x, the HRF is required. This approach is especially valuable in distributional analysis involving lifetime data, such as the lifespan distribution of a person or a component. Consequently, by taking the derivative of the logarithmic form of Equation 3

$$\frac{d}{dx}(ln(\mathcal{H}_{PRD}(x))) = \frac{\alpha\left(\frac{\alpha}{x}\right)^{-1+\theta}\theta}{x^2} + \frac{e^{-\left(\frac{\alpha}{x}\right)^{\theta}}\alpha\left(\frac{\alpha}{x}\right)^{-1+\theta}\theta}{\left(1-e^{-\left(\frac{\alpha}{x}\right)^{\theta}}\right)x^2} - \frac{\theta+1}{x} = 0. \quad (5)$$

Solution of above equation is of the form

$$x = \alpha\left(\frac{1+\theta+\theta\mathbb{W}\left(\frac{-e^{-\frac{\theta+1}{\theta}}(1+\theta)}{\theta}\right)}{\theta}\right)^{\frac{-1}{\theta}},$$

which is the mode of HRF and free from β. A closed form solution of the Equation (5) exist. Furthermore, we observed that as $x \to 0$, $(\ln(\mathcal{H}_{PRD}(0)))' = \infty$; and as $x \to \infty$, $(\ln(\mathcal{H}_{PRD}(\infty)))' = 0$, exhibiting a non-monotonically decreasing, increasing and then decreasing behaviors.

Proposition 3.1: Let X be a stochastic variable with the PDF specified in Equation (2), if and only if (iff) Equation 6 is satisfied, i.e.

$$\frac{\mathcal{H}'(x)}{(\mathcal{H}(x))^2} = \frac{\left(1+\theta+e^{\left(\frac{\alpha}{x}\right)^{\theta}}\left(-1+\left(-1+\left(\frac{\alpha}{x}\right)^{\theta}\right)\theta\right)\right)}{\left(\frac{\alpha}{x}\right)^{\theta}\beta\theta}, \quad (6)$$

where $\mathcal{H}(x)$ represents the HRF.

Proof: *Necessity*:

If X follow PRD(α,β,θ), with the PDF outlined in Equation (2), the logarithmic form of the PDF is written as

$$\begin{aligned} ln(f(x)) \;=\; & ln(\alpha) + ln(\beta) + ln(\theta) - 2ln(x) + (\theta-1)\ln\left(\frac{\alpha}{x}\right) \\ & + (\beta-1)ln\left(1-e^{-\left(\frac{\alpha}{x}\right)^{\theta}}\right) - \left(\frac{\alpha}{x}\right)^{\theta}, \end{aligned}$$

by taking the derivative of both side, we obtain

$$\frac{f'(x)}{f(x)} = \frac{\alpha\left(\frac{\alpha}{x}\right)^{-1+\theta}\theta}{x^2} + \frac{e^{-\left(\frac{\alpha}{x}\right)^{\theta}}\alpha\left(\frac{\alpha}{x}\right)^{-1+\theta}\theta}{\left(1-e^{-\left(\frac{\alpha}{x}\right)^{\theta}}\right)x^2} - \frac{\theta+1}{x} - \frac{e^{-\left(\frac{\alpha}{x}\right)^{\theta}}\alpha\left(\frac{\alpha}{x}\right)^{-1+\theta}\beta\theta}{\left(1-e^{-\left(\frac{\alpha}{x}\right)^{\theta}}\right)x^2}, \quad (7)$$

where

$$\frac{\mathcal{H}'(x)}{\mathcal{H}(x)} = \frac{\alpha\left(\frac{\alpha}{x}\right)^{-1+\theta}\theta}{x^2} - \frac{e^{-\left(\frac{\alpha}{x}\right)^{\theta}}\alpha\left(\frac{\alpha}{x}\right)^{-1+\theta}\theta}{\left(1-e^{-\left(\frac{\alpha}{x}\right)^{\theta}}\right)x^2} - \frac{\theta+1}{x},$$

and

$$\frac{f'(x)}{f(x)} = \frac{\alpha\left(\frac{\alpha}{x}\right)^{-1+\theta}\theta}{x^2}\left(1 - \frac{(\beta-1)}{\left(e^{\left(\frac{\alpha}{x}\right)^{\theta}}-1\right)}\right) - \frac{\theta+1}{x}. \tag{8}$$

Upon comparing Equation (7) with Equation (8); we derive

$$\frac{\mathcal{H}'(x)}{\mathcal{H}(x)} = \frac{\alpha\left(\frac{\alpha}{x}\right)^{-1+\theta}\theta}{x^2}\left(1 - \frac{(\beta-1)}{\left(e^{\left(\frac{\alpha}{x}\right)^{\theta}}-1\right)}\right) - \frac{\theta+1}{x} + \frac{\theta\alpha\beta e^{-(\frac{\alpha}{x})^{\theta}}}{x^2\left(1-e^{-(\frac{\alpha}{x})^{\theta}}\right)}\left(\frac{\alpha}{x}\right)^{\theta-1}.$$

After simplification, this leads to Equation (6).

Sufficiency:

Assuming that Equation 6) holds, it can be reformulated as

$$\frac{\mathcal{H}'(x)}{(\mathcal{H}(x))^2} = \frac{1}{\left(\frac{\alpha}{x}\right)^{\theta}\beta\theta}\left(1+\theta-\left(\frac{\alpha}{x}\right)^{\theta}\beta\theta + e^{\left(\frac{\alpha}{x}\right)^{\theta}}\left(\left(-1+\left(\frac{\alpha}{x}\right)^{\theta}\right)\theta\right)-1\right)+1,$$

the preceding differential equation yields

$$\mathcal{H}(u) = \frac{\theta\alpha\beta}{u^2(1-e^{-(\frac{\alpha}{u})^{\theta}})}(\frac{\alpha}{u})^{\theta-1}e^{-(\frac{\alpha}{u})^{\theta}}. \tag{9}$$

After performing the integration of the formula in Equation (9) from 0 to x, we find

$$-\ln(1-\mathcal{F}(x)) = \beta\ln(1-e^{-(\frac{\alpha}{x})^{\theta}})^{-1},$$

implying the survival function

$$\mathcal{S}(x) = (1-e^{-(\frac{\alpha}{x})^{\theta}})^{\beta}, \beta>0, \theta>0, \alpha>0, x>0.$$

3.3 *Asymptotic Versions of the PDF and HRF*

The asymptotic version of the PRD also has the two and three parameters Fréchet distributions. For this purpose, we first of all consider the CDF of the proposed model, since $\mathcal{F}(x) = 1-(1-e^{-(\frac{\alpha}{x})^{\theta}})^{\beta}$, now as $x\to\infty$ the expression $e^{-(\frac{\alpha}{x})^{\theta}} \to (1+(\frac{\alpha}{x})^{\theta})$ implies that $1-(1-e^{-(\frac{\alpha}{x})^{\theta}})^{\beta} \to 1-(\frac{\alpha}{x})^{\theta\beta}$, thus the PDF and HRF of the proposed model exhibit two parameter PRD behavior as $x\to\infty$, i.e.

$$\frac{\theta\alpha\beta}{x^2(1-e^{-(\frac{\alpha}{x})^{\theta}})^{1-\beta}}(\frac{\alpha}{x})^{\theta-1}e^{-(\frac{\alpha}{x})^{\theta}} \to \frac{\theta\alpha\beta}{x^2}(1+(\frac{\alpha}{x})^{\theta\beta})(\frac{\alpha}{x})^{\theta\beta-1}, 0<x<\infty$$

and

$$\frac{\theta\alpha\beta}{x^2}(\frac{\alpha}{x})^{\theta-1}e^{-(\frac{\alpha}{x})^{\theta}}\frac{1}{(1-e^{-(\frac{\alpha}{x})^{\theta}})}\rightarrow\frac{\theta\alpha\beta}{x^2}(1+(\frac{\alpha}{x})^{\theta\beta})(\frac{\alpha}{x})^{-1}, 0<x<\infty,$$

respectively. Also, as $x\rightarrow 0$ the expression $e^{-(\frac{\alpha}{x})^{\theta}}\rightarrow(\frac{\alpha}{x})^{-\theta}$ implies that $(1-e^{-(\frac{\alpha}{x})^{\theta}})^{\beta}\rightarrow(1-(\frac{\alpha}{x})^{-\theta})^{\beta}$, thus the PDF and HRF of the proposed model exhibit three parameter PRD's behavior as $x\rightarrow 0$, i.e.

$$\frac{\theta\alpha\beta}{x^2(1-e^{-(\frac{\alpha}{x})^{\theta}})^{1-\beta}}(\frac{\alpha}{x})^{\theta-1}e^{-(\frac{\alpha}{x})^{\theta}}\rightarrow\frac{\beta\theta\alpha}{x^2(1-(\frac{\alpha}{x})^{-\theta})^{\beta+1}}(\frac{\alpha}{x})^{-\theta-1}, 0<x<\infty$$

and

$$\frac{\theta\alpha\beta}{x^2(1-e^{-(\frac{\alpha}{x})^{\theta}})}(\frac{\alpha}{x})^{\theta-1}e^{-(\frac{\alpha}{x})^{\theta}}\rightarrow\frac{\beta\theta\alpha}{x^2}(\frac{\alpha}{x})^{-\theta-1}\frac{1}{(1-(\frac{\alpha}{x})^{-\theta})}, 0<x<\infty,$$

respectively.

3.4 *Quantile Function*

Suppose the CDF of X is given by $\mathcal{F}_X:\Re\rightarrow[0,1]$. The quantile function of X is then represented by $Q(p)$, described as

$$Q(p)=\mathcal{F}^{-1}(x)=\alpha(-ln(1-(1-p)^{\frac{1}{\beta}}))^{\frac{-1}{\theta}}, \tag{10}$$

where $p\in(0,1)$. The median when $p=0.5$ is expressed as

$$\tilde{\mu}=\alpha(-ln(1-(0.5)^{\frac{1}{\beta}}))^{\frac{-1}{\theta}}.$$

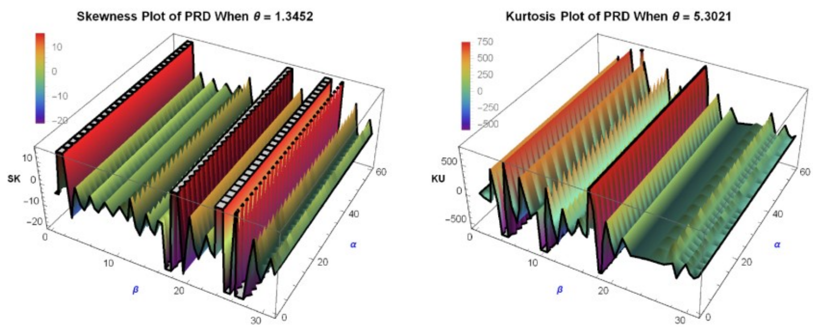

Figure 3
Skewness and Kurtosis graphs of PRD

4. Mellin and Laplace Transformation

Statistical moments are crucial for identifying probability models and are useful in characterizing the distribution. So, in this regards, the first and second statistical moments characterize the center and the variance of the model, respectively. Similarly, model skewness and kurtosis not only outline the shape of a function but also aid in illustrating the probability functions. Given these characteristics, we will define the Laplace and Mellin transformations of continuous random variables, both of which are widely used in engineering and the physical sciences. The Laplace transform is especially common in mechanical and electrical engineering, while the Mellin transform is well-known in computer science for algorithm analysis due to its scale invariance property, which is particularly useful in image recognition. Additionally, the Laplace transform can be represented as a power series, which expresses a function as a linear sum of its moments, a technique commonly employed in probability theory. However, the Mellin transform is regarded as an essential tool in analyzing the probability distributions of products of variables (variable combinations) and can be defined as follows.

Definition 4.1: The Mellin transformation of a real scalar function $\phi(x)$, where x is the real variable and s is the parameter, can be formulated as:

$$\mathcal{M}_{\phi}(s) = \int_0^{\infty} x^{s-1}\phi(x)dx, \tag{11}$$

whenever $\mathcal{M}_{\phi}(s)$ exists. The following expression represents the formula of the inverse Mellin transform

$$\phi(x) = \frac{1}{2\pi\iota}\int_{\mathfrak{L}} \mathcal{M}_{\phi}(s)x^{-s}ds, \iota = -1 \tag{12}$$

where $\mathfrak{L}$ is a suitable contour, usually $\mathfrak{L} = \{c - \iota\infty, c + \iota\infty\}$ for some real c.

Proposition 4.2: Consider X follows PRD(α, β, θ) as an absolutely continuous random variable with its CDF provided in Equation (1). The PDF described in Equation (2) holds true for for X iff the following condition is met:

$$\mathcal{M}_f(s) = \beta\alpha^{s-1}\sum_{m=0}^{\beta-1}\frac{(-\beta+1)_m}{m!}(m+1)^{\frac{s-1-\theta}{\theta}}\Gamma\left(1-\frac{s-1}{\theta}\right), \tag{13}$$

where $(a)_k = a(a+1)\ldots(a+k-1)$.

Proof: *Necessity :*

Let X follow PRD(β, λ, θ). The Mellin transform of X is given by $\mathcal{M}_f(s) = \int_0^{\infty} x^{s-1}\mathfrak{f}(x)dx$,

$$\mathcal{M}_f(s) = \alpha\beta\theta\int_0^{\infty} x^{s-1}\frac{1}{x^2(1-e^{-(\frac{\alpha}{x})^{\theta}})^{1-\beta}}(\frac{\alpha}{x})^{\theta-1}e^{-(\frac{\alpha}{x})^{\theta}}dx,$$

let $y = 1 - e^{-(\frac{\alpha}{x})^{\theta}}, -dy = \frac{\alpha\theta}{x^2}(\frac{\alpha}{x})^{\theta-1}e^{-(\frac{\alpha}{x})^{\theta}}dx$, if $x = 0, y = 1, x = \infty, y = 0$ so $x = \alpha(-ln(1-y))^{-\frac{1}{\theta}}$, then on simplification we get

$$\mathcal{M}_f(s) = \beta\alpha^{s-1}\int_0^1 (-ln(1-y))^{-(\frac{s-1}{\theta})}y^{\beta-1}dy.$$

Now, put $z = 1 - y$ and apply the binomial expansion upto $\beta - 1$ terms, i.e. $(1-z)^{\beta-1} = \sum_{m=0}^{\beta-1}\frac{(-\beta+1)_m z^m}{m!}$, we get

$$\mathcal{M}_f(s) = \beta\alpha^{s-1}\sum_{m=0}^{\beta-1}\frac{(-\beta+1)_m}{m!}\int_0^1 (-lnz)^{-(\frac{s-1}{\theta})}z^m dz,$$

on using $\int_0^1 z^m(-ln(z))^{-\frac{r}{\theta}}dz = (1+m)^{\frac{r}{\theta}-1}\Gamma(1-\frac{r}{\theta})$, see BI (107) (3), pp 551 at Gradshteyn and Ryzhik [6], we get the Equation (13).

Sufficiency:

Based on the assumption that Equation (13) is valid, it can be derived from Equation (12) that:

$$f(x) = \beta \frac{1}{2\pi\iota} \int_{\mathfrak{L}} \alpha^{s-1} \sum_{m=0}^{\beta-1} \frac{(-\beta+1)_m}{m!} (m+1)^{\frac{s-1-\theta}{\theta}} \Gamma\left(1 - \frac{s-1}{\theta}\right) ds.$$

On simplifying, we observe

$$f(x) = \beta\theta\alpha^{-1} \sum_{m=0}^{\beta-1} \frac{(-\beta+1)_m (m+1)^{\frac{-1-\theta}{\theta}}}{m!} \frac{1}{2\pi\iota} \int_{\mathfrak{L}} \alpha^{s} (m+1)^{\frac{s}{\theta}} \Gamma(1 - \frac{s-1}{\theta}) ds, \quad (14)$$

now inverse Mellin transformation can be obtained by using the **InverseMellinTransform** of Mathematica[13.0], we get

$$\frac{1}{2\pi\iota} \int_{\mathfrak{L}} \alpha^{s} (m+1)^{\frac{s}{\theta}} \Gamma(1 - \frac{s-1}{\theta}) ds = \mathrm{G}_{1,0}^{0,1}\left(\frac{x(m+1)^{-\frac{1}{\theta}}}{\alpha}, \frac{1}{\theta} \middle| -\frac{1}{\theta}\right),$$

where

$$\mathrm{G}_{m,n}^{p,q}\left(x \middle| \begin{pmatrix} a_1, a_2, \dots, a_p \\ b_1, b_2, \dots, b_p \end{pmatrix}\right) = \frac{1}{2\pi\iota} \int_{\mathfrak{L}} \frac{\prod_{j=1}^{m} \Gamma(b_j - s) \prod_{j=1}^{n} \Gamma(1 - a_j + s)}{\prod_{j=m+1}^{q} \Gamma(1 - b_j + s) \prod_{j=n+1}^{p} \Gamma(a_j - s)} x^{s} ds.$$

Also by using Mathematica[13.0] built in command **MeijerGToHypergeometricPFQ**, we obtain

$$\mathrm{G}_{1,0}^{0,1}\left(\frac{x(m+1)^{-\frac{1}{\theta}}}{\alpha}, \frac{1}{\theta} \middle| -\frac{1}{\theta}\right) = \theta e^{-\left(\frac{(m+1)^{-\frac{1}{\theta}} x}{\alpha}\right)} \left(\frac{(m+1)^{-\frac{1}{\theta}} x}{\alpha}\right)^{(-1-\frac{1}{\theta})\theta},$$

which on incorporating into Equation (14) yields Equation (2).

Corollary 4.3: *On replacing $s-1$ by r in Equation (13), we get the r^{th} moment about origin as*

$$\mu_r' = \beta\alpha^{r} \Gamma(1 - \frac{r}{\theta}) \sum_{m=0}^{\beta-1} \frac{(-\beta+1)_m}{m!} (1+m)^{\frac{r}{\theta}-1},$$

for which $\Gamma(a) = \int_0^\infty t^{a-1} e^{-t} dt$ denotes the gamma function. Furthermore, skewness (a measure of asymmetry) and kurtosis (a measure of peakedness) can be derived from moment ratios, although these ratios do not have closed-form expressions. Nonetheless, their graphical representations are shown in Figure 3, which illustrates negative and positive skewness, symmetry, as well as leptokurtic, mesokurtic, and platykurtic behaviors, respectively.

Proposition 4.4: If X follows $\mathrm{PRD}(\alpha, \beta, \theta)$, its Laplace transformation is expressed as

$$\mathfrak{L}_f(s) = \beta \sum_{r=0}^{\infty} \sum_{m=0}^{\infty} \frac{(-\beta+1)_m (-\alpha s)^{r}}{m! r!} (1+m)^{\frac{r}{\theta}-1} \Gamma\left(1 - \frac{r}{\theta}\right). \quad (15)$$

Proof: As X follows $\mathrm{PRD}(\alpha, \beta, \lambda, \theta)$ and by using the definition $\mathfrak{L}_f(s) = \int_0^\infty e^{-sx} f(x) dx$, the Laplace transform of X is expressed as

$$\mathfrak{L}_f(s) = \int_0^\infty e^{-sx} \frac{\theta\alpha\beta}{x^2(1-e^{-(\frac{\alpha}{x})^\theta})^{1-\beta}} (\frac{\alpha}{x})^{\theta-1} e^{-(\frac{\alpha}{x})^\theta} dx.$$

Let $y = 1 - e^{-(\frac{\alpha}{x})^\theta}, -dy = \frac{\alpha\theta}{x^2}(\frac{\alpha}{x})^{\theta-1} e^{-(\frac{\alpha}{x})^\theta} dx$, and $x = \alpha(-ln(1-y))^{-\frac{1}{\theta}}$, then on simplification we get

$$\begin{aligned}\mathfrak{L}_f(s) &= \beta \int_0^1 y^{\beta-1} e^{-\alpha s((-ln(1-y))^{-\frac{1}{\theta}})} dy \\ &= \beta \sum_{r=0}^\infty \frac{(-\alpha s)^r}{r!} \int_0^1 y^{\beta-1}(-ln(1-y))^{-\frac{r}{\theta}} dy.\end{aligned}$$

Now, substitute $1 - y = z$, we get

$$\mathfrak{L}_f(s) = \beta \sum_{r=0}^\infty \frac{(-\alpha s)^r}{r!} \int_0^1 (1-z)^{\beta-1}(-ln(z))^{-\frac{r}{\theta}} dz.$$

On using binomial expansion $(1-z)^a = \sum_{m=0}^\infty \frac{(-a)_m z^m}{m!}$, we get

$$\mathfrak{L}_f(s) = \beta \sum_{r=0}^\infty \sum_{m=0}^\infty \frac{(-\beta+1)_m(-\alpha s)^r}{m!r!} \int_0^1 z^m(-ln(z))^{-\frac{r}{\theta}} dz,$$

by using $\int_0^1 z^m(-ln(z))^{-\frac{r}{\theta}} dz = (1+m)^{\frac{r}{\theta}-1}\Gamma(1-\frac{r}{\theta})$, see BI (107) (3), pp 551 at Gradshteyn and Ryzhik [6], we get Equation (15).

Corollary 4.5: *On replacing $-s$ by t in Equation (15), then the moment generating function is expressed as*

$$\mathcal{M}_X(t) = \beta \sum_{r=0}^\infty \sum_{m=0}^\infty \frac{(-\beta+1)_m(\alpha t)^r}{m!r!} (1+m)^{\frac{r}{\theta}-1} \Gamma\left(1-\frac{r}{\theta}\right).$$

5. Order Statistics with Asymptotic Distributions

In studying extreme value distribution, let the sample elements be $X_1, X_2, \ldots, X_n$. The r^{th} order statistics is denoted by $Y_r = X_{r:n}$, and the PDF of Y_r is given by

$$\psi(y_r;\Theta) = \frac{n!}{(r-1)!(n-r)!} (\mathcal{F}_{\mathrm{PRD}}(y_r|\Theta))^{r-1}(y_r)(\mathcal{S}_{\mathrm{PRD}}(y_r|\Theta))^{n-r} f_{\mathrm{PRD}}(y_r|\Theta), y_r \in \mathbb{R}. \tag{16}$$

On substituting the expressions for CDF of the PRD distribution into Equation (16), we get

$$\begin{aligned}\psi(y_r;\alpha,\beta,\theta) &= \frac{n!\alpha\beta\theta}{(r-1)!(n-r)!y_r^2} \left(1-(1-e^{-(\frac{\alpha}{y_r})^\theta})^\beta\right)^{r-1} (\frac{\alpha}{y_r})^{\theta-1} e^{-(\frac{\alpha}{y_r})^\theta} \\ &\quad \times (1-e^{-(\frac{\alpha}{y_r})^\theta})^{\beta(n-r+1)-1},\end{aligned}$$

where $y_r \in \mathbb{R}, \alpha, \beta, \theta > 0$. Similarly, the smallest and largest order statistics are expressed as

$$\psi(y_1;\alpha,\beta,\theta) = \frac{n\alpha\beta\theta}{y_1^2} (\frac{\alpha}{y_1})^{\theta-1} e^{-(\frac{\alpha}{y_1})^\theta} (1-e^{-(\frac{\alpha}{y_1})^\theta})^{n\beta-1},$$

where $y_1 \in \mathbb{R}, \alpha, \beta, \theta > 0$, and

$$\psi(y_n;\alpha,\beta,\theta)=\frac{n\alpha\beta\theta}{y_n^2(1-e^{-(\frac{\alpha}{y_n})^\theta})^{1-\beta}}\left(1-(1-e^{-(\frac{\alpha}{y_n})^\theta})^\beta\right)^{n-1}(\frac{\alpha}{y_n})^{\theta-1}e^{-(\frac{\alpha}{y_n})^\theta},$$

where $y_n\in\mathbb{R},\alpha,\beta,\theta>0$. Now, let $W_n=X_{n:n}$ and $w_n=X_{1:n}$, representing the largest and smallest values, respectively, in a random sample of n observations. To determine the distribution of the maxima, we refer to Theorem (1.6.2) (see Leadbetter, Lindgren, and Rootzen [12]), which after using L'H$\hat{o}$pital's rule, yields

$$\lim_{t\to\infty}\frac{\mathcal{F}(tx)}{\mathcal{F}(t)}=\lim_{t\to\infty}\frac{xf(tx)}{f(t)}=x^{-2\theta},$$

with standarized form expressed as $e^{x^{-2\theta}}$, which is Fréchet (type -II) distribution. If $\tilde{a}_n>0,\tilde{b}_n>0,\tilde{c}_n>0$ and $\tilde{d}_n>0$ are the norming constants, then, based on Theorem (1.6.3) from Leadbetter, Lindgren, and Rootzen [12], we get

$$P\{\tilde{a}_n(W_n-\tilde{b}_n)\le x\}\to e^{-\frac{1}{x^{2\theta}}}.$$

As a result, the asymptotic distribution of the sample maxima lies in the domain of attraction of the Fréchet distribution. Similarly, to find the distribution of the minima, we utilize Theorem 1.6.2 as outlined by Leadbetter, Lindgren, and Rootzen [12], which states that

$$\lim_{t\to 0}\frac{1-\mathcal{F}(tx+\omega)}{1-\mathcal{F}(t+\omega)}=1,$$

$$P\{\tilde{c}_n(w_n-\tilde{d}_n)\le x\}\to 1-e^{-1},$$

as $n\to\infty$. Accordingly, the sample minimum is attracted to the domain of the Weibull distribution.

6. Estimation of Parameters

The AMF series is treated as a random sample drawn from a population of flood values, whose distribution is characterized by a probability density function (PDF) that typically relies on only a few parameters. Generally, distributions with two or three parameters are preferred. The selection of a probability model and the estimation of its parameters can be approached using either non-Bayesian or Bayesian methods. While Bayesian methods are often applied in regional analyses due to their ability to incorporate subjective prior distributions, they can significantly influence the choice of posterior probability models and often involve high computational costs-particularly for models with many parameters, see SAS Institute Inc [21]. Therefore, in this study, we focus on non-Bayesian approaches such as the probability-weighted moments (PWMs) and maximum likelihood (ML) methods, which are discussed in the following subsections.

6.1 *L-Moments*

Let $X_1,X_2,\ldots,X_i,\ldots,X_n$ be identically and independently distributed stochastic variates each with PDF as defined in Equation (2), CDF as given in Equation (1), and the quantile function $Q(u)$. The PWMs method can then be presented in the following form

$$M_{p,u,s}=\mathbb{E}(X(\mathcal{F}(X))^u(1-\mathcal{F}(X))^s).$$

For the PRD, it can be written as

$$M_{p,u,s}=\int_0^\infty x^p(1-e^{-(\frac{\alpha}{x})^\theta})^{s\beta}\left(1-(1-e^{-(\frac{\alpha}{x})^\theta})^\beta\right)^u\frac{\theta\alpha\beta}{x^2}(\frac{\alpha}{x})^{\theta-1}e^{-(\frac{\alpha}{x})^\theta}(1-e^{-(\frac{\alpha}{x})^\theta})^{\beta-1}dx,$$

which on using $(1-z)^s=\sum_{k=0}^{s}\frac{(-s)_k z^k}{k!}$ and substituting $1-(1-e^{-(\frac{\alpha}{x})^\theta})^\beta=y$, this yields the resultant expression as

$$M_{p,u,s}=\int_0^1(\alpha(-ln(1-(1-y)^{1/\beta}))^{-1/\theta})^p(1-y)^s y^u dy.$$

Similarly substituting $1-(1-y)^{1/\beta}=z\Rightarrow(1-y)=(1-z)^\beta\Rightarrow dy=\beta(1-z)^{\beta-1}dz,$ which yields the resultant expression as

$$M_{p,u,s}=\alpha^p\beta\int_0^1((-ln(z))^{-p/\theta})(1-z)^{s\beta+\beta-1}(1-(1-z)^\beta)^u dz.$$

On taking $p=1,u=0$ and $s=k$, we get

$$\alpha_k=M_{1,0,k}=\alpha\beta\int_0^1((-ln(z))^{-1/\theta})(1-z)^{k\beta+\beta-1}dz,$$

$$\alpha_k=\alpha\beta\sum_{m=0}^{\beta(k+1)-1}\frac{(-\beta(k+1)+1)_m}{m!}\int_0^1((-ln(z))^{-1/\theta})z^m dz,$$

which on simplification, it yields

$$\alpha_k=\alpha\beta\Gamma(1-\frac{1}{\theta})\sum_{m=0}^{\beta(k+1)-1}\frac{(-\beta(k+1)+1)_m(m+1)^{\frac{1}{\theta}}}{(m+1)m!},$$

where $\int_0^1((-ln(z))^{-1/\theta})z^m dz=(m+1)^{\frac{1}{\theta}-1}\Gamma(1-\frac{1}{\theta})$. However, PWMs are not straightforward to interpret as direct measures of a probability distribution's scale and shape. This descriptive information is instead embedded in specific linear combinations of PWMs. Accordingly, the L-moments, in terms of PWMs, are defined as follows:

$$\lambda_{r+1}=(-1)^r\sum_{k=0}^{r}p*_{r,k}\,\alpha_k, \tag{17}$$

where $p*_{r,k}=\frac{(-1)^{r-k}(r+k)!}{(k!)^2(r-k)!}$. Now, on substituting α_k in Equation (17) we get

$$\alpha_k=\alpha\beta\Gamma(1-\frac{1}{\theta})\sum_{m=0}^{\beta(k+1)-1}\frac{(-\beta(k+1)+1)_m(m+1)^{\frac{1}{\theta}}}{(m+1)m!}.$$

The L-moments for the PRD can be expressed as

$$\lambda_{r+1}=\alpha\beta\Gamma(1-\frac{1}{\theta})\sum_{k=0}^{r}\sum_{m=0}^{\beta(k+1)-1}\frac{(-1)^{2r-k}(r+k)!}{(k!)^2(r-k)!}\frac{(-\beta(k+1)+1)_m(m+1)^{\frac{1}{\theta}}}{(m+1)m!},$$

where $r=0,1,2,\ldots$, which yields for

$$r=0\Rightarrow\lambda_1=\alpha\beta\Gamma(1-\frac{1}{\theta})\sum_{m=0}^{\beta-1}\frac{(-\beta+1)_m(m+1)^{\frac{1}{\theta}}}{(m+1)m!},\beta\geq1,$$

$$r=1\Rightarrow\lambda_2=\alpha\beta\Gamma(1-\frac{1}{\theta})\{\sum_{m=0}^{\beta-1}\frac{(-\beta(k+1)+1)_m(m+1)^{\frac{1}{\theta}}}{(m+1)m!}$$

$$-2\sum_{m=0}^{2\beta-1}\frac{(-2\beta+1)_m(m+1)^{\frac{1}{\theta}}}{(m+1)m!}\},$$

$$r = 2 \Rightarrow \lambda_3 \;=\; \alpha\beta\Gamma(1-\tfrac{1}{\theta})\{\sum_{m=0}^{\beta-1} \frac{(-\beta+1)_m(m+1)^{\frac{1}{\theta}}}{(m+1)m!} - 6\sum_{m=0}^{2\beta-1} \frac{(-2\beta+1)_m(m+1)^{\frac{1}{\theta}}}{(m+1)m!} + 6\sum_{m=0}^{3\beta-1} \frac{(-3\beta+1)_m(m+1)^{\frac{1}{\theta}}}{(m+1)m!}\},$$

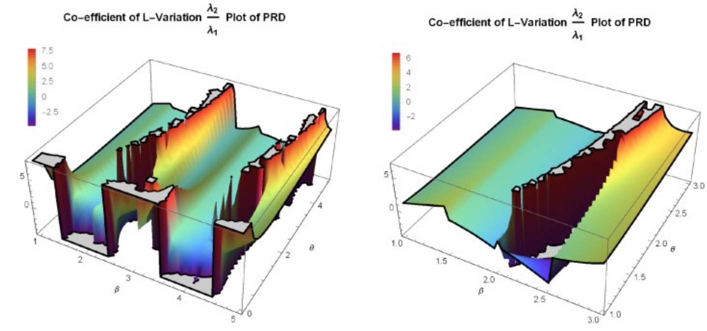

Figure 4
Coefficient of L-variation graphs of PRD

and

$$r = 3 \Rightarrow \lambda_4 \;=\; \alpha\beta\Gamma(1-\tfrac{1}{\theta})\{\sum_{m=0}^{\beta-1} \frac{(-\beta+1)_m(m+1)^{\frac{1}{\theta}}}{(m+1)m!} - 12\sum_{m=0}^{2\beta-1} \frac{(-2\beta+1)_m(m+1)^{\frac{1}{\theta}}}{(m+1)m!} + 30\sum_{m=0}^{3\beta-1} \frac{(-3\beta+1)_m(m+1)^{\frac{1}{\theta}}}{(m+1)m!} - 20\sum_{m=0}^{4\beta-1} \frac{(-4\beta+1)_m(m+1)^{\frac{1}{\theta}}}{(m+1)m!}\}.$$

From the above expression we can define the L-moment ratios as $\tau_r = \frac{\lambda_r}{\lambda_2}$, $r = 3,4, \dots$. Therefore, for the PRD we have L-moments ratio and coefficient of L-variations as

$$\tau_3 = \frac{\lambda_3}{\lambda_2} = \frac{6\beta_2 - 6\beta_1 + \beta_0}{6\beta_1 - \beta_0}, \text{and } \tau = \frac{\lambda_2}{\lambda_1} = \frac{2\beta_1 - \beta_0}{\beta_0},$$
$$\tau_4 = \frac{\lambda_4}{\lambda_2} = \frac{20\beta_3 - 30\beta_2 + 12\beta_1 - \beta_0}{6\beta_1 - \beta_0},$$

respectively.

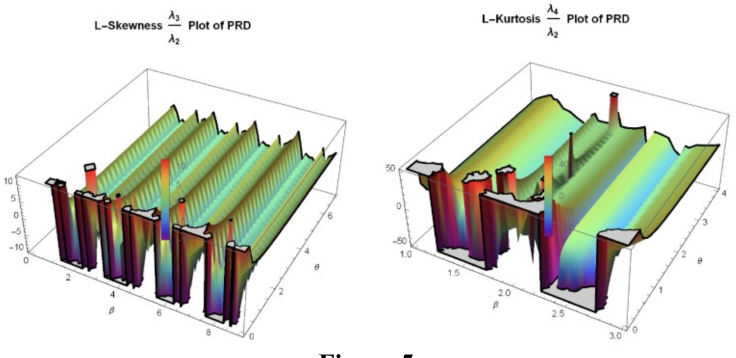

Figure 5
L-Moments Ratio graphs of PRD

As discussed earlier, it is obvious from Figure 5 that L-Skewness ($\tau_3 = \frac{\lambda_3}{\lambda_2}$) lies between -10 to 10, indicating that the PRD is a symmetric, negatively, and positively skewed distribution. Similalry, the L-Kurtosis $\tau_4 = \frac{\lambda_4}{\lambda_2}$ implies mesokurtic to leptokurtic behavior. Further, all L-moment ratios expressions are free from α but depend on β and θ. Moreover, the cofficient of L-variations exhibits low values for smaller β and larger values for higher β, which is portrayed in Figure 4.

6.2 *The Maximum Likelihood Approach*

Maximum Likelihood Estimation (MLE) is one of the most widely used methods for parameter estimation. Its asymptotic theory provides straightforward calculations that perform well even with limited sample data. Statisticians commonly use MLE to estimate quantities such as the density of a test statistic, which depends on sample size, in order to obtain more accurate estimators of distribution parameters. The computations involved in deriving MLEs within distribution theory can be handled analytically or numerically. In this subsection, we focus on estimating parameters using the MLE method based on the entire sample. Let $x_1, \ldots, x_n$ be a stochastic realization of size n from the PRD distribution, as defined in Equation (2). The log-likelihood function corresponding to the PRD can be expressed as

$$\ell_n(\Theta) = n ln(\alpha\beta\theta) - 2\sum_{i=1}^{n} ln(x_i) - (\theta - 1)\sum_{i=1}^{n} ln(\frac{\alpha}{x_i})$$
$$-\sum_{i=1}^{n} (\frac{\alpha}{x_i})^{\theta} - \sum_{i=1}^{n} \left(1 - e^{-(\frac{\alpha}{x_i})^{\theta}}\right)^{\beta}, \tag{18}$$

by taking the partial derivatives of Equation (18) w. r. t α, θ and β, respectively, and setting the resulting expressions equal to zero, we obtain the following system of equations:

$$\frac{\partial \ell_n(\Theta)}{\partial \alpha} = \frac{n}{\alpha} + \frac{n(-1+\theta)}{\alpha} - \sum_{i=1}^{n} \frac{\theta\left(\frac{\alpha}{x_i}\right)^{-1+\theta}}{x_i} + (\beta - 1)\sum_{i=1}^{n} \frac{e^{-\left(\frac{\alpha}{x_i}\right)^{\theta}} \theta\left(\frac{\alpha}{x_i}\right)^{-1+\theta}}{\left(1-e^{-\left(\frac{\alpha}{x_i}\right)^{\theta}}\right)x_i} = 0, \tag{19}$$

$$\frac{\partial \ell_n(\Theta)}{\partial \beta} = \frac{n}{\beta} + \sum_{i=1}^{n} \left(1 - e^{-(\frac{\alpha}{x_i})^{\theta}}\right) = 0, \tag{20}$$

and

$$\frac{\partial \ell_n(\Theta)}{\partial \theta} = \frac{n}{\theta} + \sum_{i=1}^{n} ln\left[\frac{\alpha}{x_i}\right] - \sum_{i=1}^{n} ln\left[\frac{\alpha}{x_i}\right]\left(\frac{\alpha}{x_i}\right)^{\theta} + (\beta - 1)\sum_{i=1}^{n} \frac{e^{-\left(\frac{\alpha}{x_i}\right)^{\theta}} ln\left[\frac{\alpha}{x_i}\right]\left(\frac{\alpha}{x_i}\right)^{\theta}}{1-e^{-\left(\frac{\alpha}{x_i}\right)^{\theta}}} = 0. \tag{21}$$

Because these equations cannot be solved algebraically, statistical tools like Mathematica [13.0] are employed. The variance-covariance matrix and the confidence intervals of the estimators are determined using the information matrix, which is computed by taking the expectation of the second-order derivatives from Equations (19), (20), and (21). This leads to the following expression:

$$\mathbb{I}_{\hat{\alpha},\hat{\beta},\hat{\theta}} = \begin{array}{c} \\ \hat{\alpha} \\ \hat{\beta} \\ \hat{\theta} \end{array} \begin{array}{c} \begin{array}{ccc} \hat{\alpha} & \hat{\beta} & \hat{\theta} \end{array} \\ \begin{pmatrix} -\mathbb{E}\left(\frac{\partial^2 \ell(\Theta)}{\partial \alpha^2}\right) & -\mathbb{E}\left(\frac{\partial^2 \ell(\Theta)}{\partial \alpha\, \partial \beta}\right) & -\mathbb{E}\left(\frac{\partial^2 \ell(\Theta)}{\partial \alpha\, \partial \theta}\right) \\ -\mathbb{E}\left(\frac{\partial^2 \ell(\Theta)}{\partial \alpha \beta}\right) & -\mathbb{E}\left(\frac{\partial^2 \ell(\Theta)}{\partial \beta^2}\right) & -\mathbb{E}\left(\frac{\partial^2 \ell(\Theta)}{\partial \beta\, \partial \theta}\right) \\ -\mathbb{E}\left(\frac{\partial^2 \ell(\Theta)}{\partial \theta\, \partial \lambda}\right) & -\mathbb{E}\left(\frac{\partial^2 \ell(\Theta)}{\partial \theta\, \partial \beta}\right) & -\mathbb{E}\left(\frac{\partial^2 \ell(\Theta)}{\partial \theta^2}\right) \end{pmatrix} \end{array}.$$

Considering the regularity conditions, the PRD (α, β, θ) model satisfies the regularity conditions outlined by (Rohatgi and Saleh [18], pp. 419). Consequently, the confidence interval belt of the MLEs vector $\widehat{\Theta}$=($\hat{\alpha}$, $\hat{\beta}$, $\hat{\theta}$) is both consistent and asymptotically normal. In other words, $\sqrt{n}\left[\widehat{\Theta}^T - \Theta^T\right] \sim \mathrm{TVN}[0, \mathbb{I}^{-1}]$, where $\mathbb{I}^{-1}$ represents the inverse of the expected Fisher information matrix, which is used to generate the variance-covariance matrix based on the expectation of the second-order derivatives of the log-likelihood.

7. Discussion to Flood Data Application

7.1 *Flood Frequency Analysis*

Flood measures can be analyzed using either the annual maximum series (AMS) or partial-duration series (PDS). The AMS focuses on the highest flood peak observed in each year. In contrast, the PDS includes all flood peaks that meet or exceed a specified base flood level. As a result, for $n -$year data, it may produce m peaks, where $m < n$. In this context, Bulletin Nos. 15, 17, 17A, 17B, and 17C provide a set of guidelines for flood frequency analysis, issued by the Water Resources Council (USWRC), as detailed by England et al. [5]. According to these guidelines, flood frequency estimates are suitable for floods with an annual exceedance probability (AEP) of 0.10 or lower, i.e., $(Q_p \leq Q_{0.10})$, where the $\mathrm{AEP}_p \leq 0.1$, such as 0.01. Consequently, AMS offers a reliable sample for this type of analysis. Furthermore, there is minimal difference in AEP estimates between AMS and PDS for these quantiles, as noted by England et al. [5]. Additionally, AMS is preferred for its ease of use and long-term availability. On the other hand, PDS may be affected by imperfect records, especially when defining the threshold(s) for PDS.

7.2 *Data Sources and Competing Models*

Flood frequency analysis is typically based on three core data types: instrumental records, documented historical floods, and paleohydrologic and botanical indicators. In this research, we adopted the systematic records and summarize them in Table-3, however the flood measurements are listed below. Moreover, for an in-depth analysis of model performance and realistic return period estimation, the PRD was evaluated in comparison with established three-parameter distributions, specifically Kappa(3) and Gamma(3). Similarly, two-parameter distributions, including Weibull (WD(2)), Gamma (GD(2)), Extreme Values (EV(2)), Log Logistic (LLD(2)) , Log Normal (LN(2)) and Gumbel (GuD(2)).

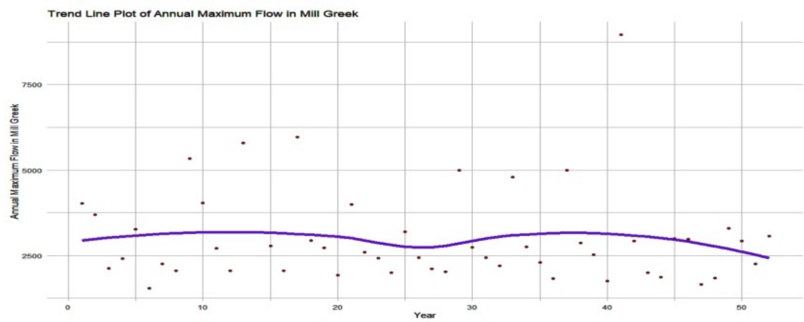

Figure 6
Trend line Plot of the Data Set-I

For comparison purpose we have studied two real-world flood data sets constituting AMF series, the first one measures the flow data for Mill Creek (Station 93) near Manhattan, IN for the period of 1940-1991 with measurements in cubic feet per second (cfs) taken from Hamed and Rao [7], and these data's values are: 4020, 3690, 2130, 2410, 3270, 1540, 2250, 2060, 5340, 4040, 2710, 2050, 5800, 3180, 2780, 2050, 5960, 2940, 2730, 1930, 4000, 2600, 2430, 1990, 3200, 2440, 2110, 2030, 5000, 2740, 2440, 2190, 4800, 2750, 2290, 1830, 5000, 2860, 2520, 1750, 8960, 2920, 2000, 1870, 3000, 2980, 1650, 1840, 3290, 2930, 2260, 3060.

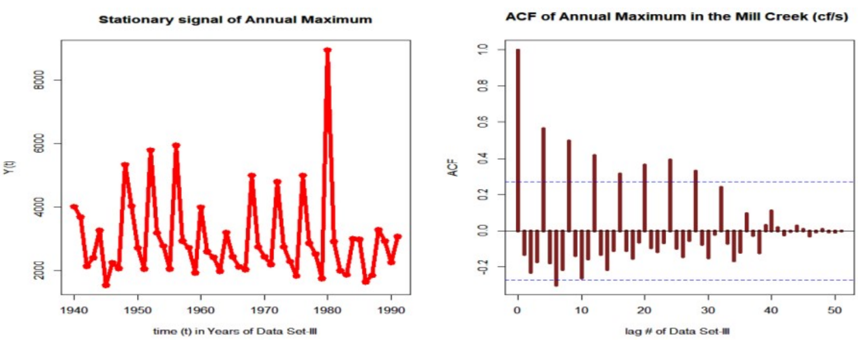

Figure 7
Time Series and ACF Plots for the Data Set-I

The second data set, which measures the peak in cubic meter per second (m^3/s), was obtained from $https://nrfa.ceh.ac.uk/data/station/peakflow/39008$. The National River Flow Archive (NRFA) provides access to its peak flow data of 96 stations, and the values of such data are: 54.234, 81.635, 54.349, 78.382, 52.494, 59.305, 78.484, 51.479, 48.819, 52.674, 79.532, 65.128, 49.693, 74.867, 50.165, 49.347, 48.683, 72.413, 53.646, 47.325, 50.126, 54.261, 50.967, 64.294, 65.318, 64.898, 83.066, 54.338, 50.749, 56.469, 53.75, 83.059, 91.572, 72.319, 51.751, 62.626, 75.505, 62.157, 50.001, 57.514, 62.028, 56.744, 70.192, 56.502, 91.796, 70.87, 51.12, 55, 50.9, 49, 59.792, 55.786, 79.838, 63.85, 51.751, 76.892, 102.054, 49.259, 49.179, 56.34, 87.587, 59.024, 75.38, 57.788, 56.754, 54.145, 75.795, 54.746, 59.529, 60.135, 52.464, 51.439, 51.896, 66.552, 48.935, 48.781, 96.4, 48.366, 50.741, 97.989, 68.151, 76.208, 52.154, 64.358, 68.661, 51.555, 107.355, 99.092, 70.097, 54.992, 77.875, 76.292, 59.542, 50.16, 47.211, 51.5.

Table 1

Nonparametric Tests summary

Data Sets	KPSS-test	$p-value$	MK-test	$p-value$	SW-test	$p-value$
I	0.1004	0.1000	-0.7891	0.4300	0.7879	0.0000
II	0.1688	0.1000	-0.7168	0.4735	0.8652	0.0000

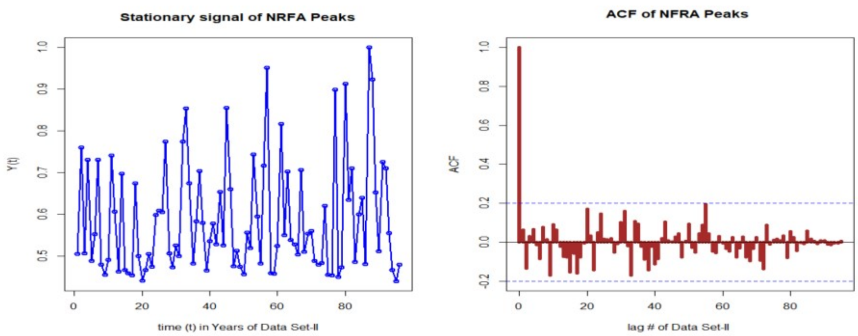

Figure 8
Time Series and ACF Plots for the Data Set-II

Based on Table-1, the Shapiro-Wilk (SW) test for normality indicates that the data set is not normal at one percent levels of significance, thus indicating the presence of outliers, which can be visualized from QQ-plots portrayed in Figures 10 and 11. Since all points do not fall along this straight line, so we can not assume normality.

7.3 *Assumptions and Notable Issues in the Dataset*

The primary expectation for statistical analysis is that the flood data collected should be reliable and reflect a representative random sample of homogeneous events over time. As such, evaluating the appropriateness and relevance of flood records is an essential part of flood frequency analysis. In general, a time series of annual peak-flow estimates is treated as a random sample of independent and identically distributed variables. The peak-flow time series is presumed to accurately represent the population of future flood events. In principle, the stochastic process generating floods is assumed to be stationary, meaning it remains consistent over time.

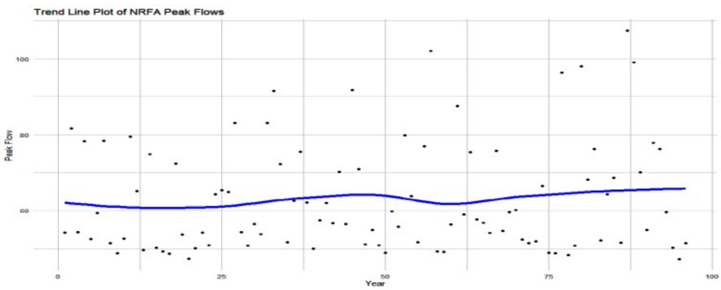

Figure 9
Trend line Plot for the Data Set-II

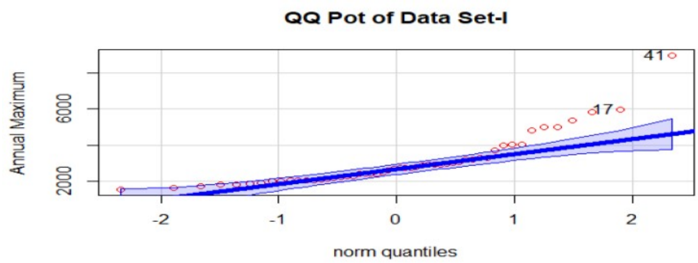

Figure 10
QQ-Plot for the Data Set-I

Identifying non-stationary patterns in peak-flow series can be difficult. To address this, we applied the Kwiatkowski-Phillips-Schmidt-Shin (KPSS) test, which tests the null hypothesis that a time series is stationary around a deterministic trend, against the alternative hypothesis of non-stationarity. Additionally, we used the Mann-Kendall (MK) test to assess the independence and detect any monotonic upward or downward trends in the AMS over time. From Table-1, it is evident that KPSS, MK and SW tests provide strong evidence in favor of level stationarity (which is also clear from Figures 7 and 8 for plots of both time series data sets), independence and identical realizations, and non-normal behavior.

Table 2

Kendall's rank correlation (τ) test summary

Data Sets	$\hat{\tau}$	T-test	$p-value$
I	-0.0762	-0.7970	0.4254
II	0.0388	0.5602	0.5753

Kendall's rank correlations (τ) are also calculated for determining the trends in an AMS, which are portrayed in Figures 6 and 9, indicating a negative and positive trend between years and volume for data set-I and -II respectively, with higher $p-values$ indicating no monotonic relationship between them, as shown in Table-2

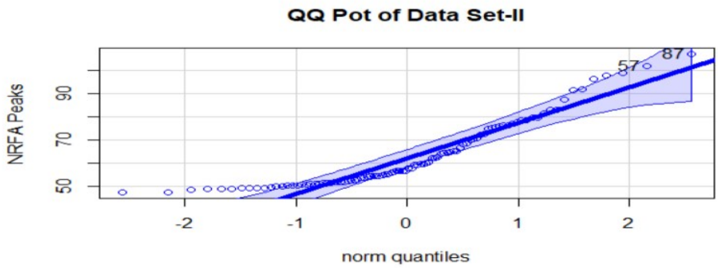

Figure 11
QQ-Plot for the Data Set-II

In addition, time series and autocorrelation plots are portrayed in Figures 7 and 8. Notably, the stationary signal (left) in Figures 7 and 8 results in few significant lags (right panel) that exceed the confidence interval of the ACF (blue dashed line). Intuitively, we can realize and summarize from the ACFs plots that the signal, on the left panel, is stationary because the lags that die out.

Table 3
Descriptive summary of Data

Data Set	Sample Size	Mean	Median	S.D	SK	KU
I	52	3011.73	2720.00	1363.71	2.1199	8.6042
II	96	62.9785	57.134	14.4087	1.13741	3.53627

Table 4(a)
MLEs and Goodness-of-Fit measures of the Data Set-I

Distribution	$\hat{\alpha}$	$\hat{\theta}$	$\hat{\beta}$	A_0^*	W_0^*	KS	$p-value$
PRD	2454.0567	3.2076	1.1412	0.2109	0.0348	0.0728	0.9574
Kappa(3)	4.4955	0.9577	2614.65	33.9922	7.3047	0.7408	0.0000
GD(3)	74.8171	0.0024	0.3089	1.0732	0.1750	0.1326	0.3552
WD(2)	2.3071	3404.18	-	2.6105	0.4431	0.1927	0.0525
GD(2)	6.7968	443.11	-	1.5066	0.2559	0.1549	0.1903
EVD(2)	2479.07	804.21	-	0.8917	0.1253	0.1016	0.6926
LLD(2)	4.9309	2693.13	-	0.5937	0.0595	0.0683	0.9263
LND(2)	7.9349	0.3668	-	0.9190	0.1479	0.1236	0.4427
GuD(2)	3798.06	2001.99	-	5.9406	1.1005	0.2765	0.0011

While discussing the assumption of flood data sets we have observed that the selected data sets follow the usual assumptions like stationarity, independence, and trend nature. At this point, we will assess the goodness-of-fit statistics for the proposed model alongside the competing models.

The selected data sets are leptokurtic and positively skewed, and for the PRD model, minimum goodness-of-fit measures with high p-values, as indicated in Tables 4(a) and 5(a). This supports the appropriateness of the proposed model, suggesting that the PRD is the best choice for such dataset. Additionally, the histograms in Figure 12 and the information criteria presented in Tables 4(b) and 5(b) further reinforce the model's suitability, demonstrating minimal information loss and the best fit for the PRD model.

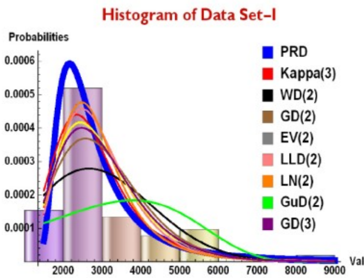

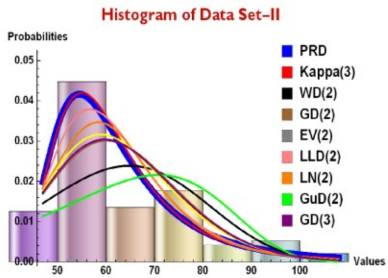

Figure 12
Histogram for the Data Set-I and -II

The information matrix is an essential measure that must be estimated in order to construct confidence intervals around point estimates. It is derived from the matrix of second derivatives of the log-likelihood and serves as the foundation for the variance-covariance matrix. This square matrix includes the variances and covariances of the different variables. The diagonal elements indicate the variances of the individual variables, while the off-diagonal elements represent the covariances between all possible variable pairs. This matrix is a valuable tool for assessing the relationships between different structures or variables. It aids in understanding patterns and dependencies in data, facilitating tasks such as dimensionality reduction, clustering, or regression analysis.

Table 4(b)
Information criterion for the Data Set-I

Distribution	$-l$	AIC	AICC	BIC	HQIC	CAIC
PRD	429.7096	865.0030	865.5030	870.8570	861.7510	865.5030
Kappa(3)	434.2351	870.8700	871.3700	875.7300	874.6200	871.3700
GD(3)	435.2270	878.4540	879.3050	886.2590	873.2020	879.3050
WD(2)	444.8790	893.7580	894.0020	897.6600	892.5060	894.0020
GD(2)	437.8450	879.6910	879.9360	883.5930	878.4390	879.9360
EVD(2)	434.3140	872.6290	872.8740	876.5310	871.3770	872.8740
LLD(2)	433.7180	871.4350	871.6800	875.3380	870.1840	871.6800
LND(2)	434.2490	872.4980	872.7430	876.4000	871.2460	872.7430
GuD(2)	467.7230	939.4460	939.6910	943.3480	938.1940	939.6910

In this context, we have also computed the variance-covariance matrix for the PRD. The confidence interval bands for the estimates of $\hat{\alpha}$, $\hat{\beta}$ and $\hat{\theta}$ for the data sets can be observed in Figures 13, 14, and 15, respectively.

$$\mathbb{COV}_{\mathrm{I}} = \begin{array}{c} \\ \hat{\alpha} \\ \hat{\beta} \\ \hat{\theta} \end{array} \begin{array}{c} \begin{array}{ccc} \hat{\alpha} & \hat{\beta} & \hat{\theta} \end{array} \\ \begin{pmatrix} 10021.2 & -24.014 & 97.7304 \\ -24.014 & 0.02504 & 0.1159 \\ 97.7304 & 0.1159 & 0.1099 \end{pmatrix} \end{array},$$

$$\mathbb{COV}_{\mathrm{II}} = \begin{array}{c} \\ \hat{\alpha} \\ \hat{\beta} \\ \hat{\theta} \end{array} \begin{array}{c} \begin{array}{ccc} \hat{\alpha} & \hat{\beta} & \hat{\theta} \end{array} \\ \begin{pmatrix} 0.7952 & -0.1323 & \hat{\alpha}1.9784 \\ -0.1323 & 0.0082 & 0.0864 \\ 1.9784 & 0.0864 & 0.3115 \end{pmatrix} \end{array}.$$

Table 5(a)

MLEs and Goodness-of-Fit measures of the Data Set-II

Distribution	$\hat{\boldsymbol{\alpha}}$	$\hat{\boldsymbol{\theta}}$	$\hat{\boldsymbol{\beta}}$	$\mathbf{A}_0^*$	$\mathbf{W}_0^*$	**KS**	$\boldsymbol{p-value}$
PRD	55.2224	6.6609	0.8887	1.6234	0.2651	0.1060	0.2358
Kappa(3)	687.6587	0.0009	152.93	1.9240	0.2988	0.1061	0.2357
GD(3)	38.8770	0.4668	0.7473	3.1205	0.5129	0.1482	0.0307
WD(2)	4.3382	68.8192	-	4.4453	0.7276	0.1771	0.0051
GD(2)	21.7629	2.8938	-	3.2649	0.5413	0.1520	0.0248
EVD(2)	56.7169	9.7213	-	2.6260	0.4097	0.12832	0.0875
LLD(2)	1.7122	51042.47	-	2.7160	0.3742	0.1216	0.1202
LND(2)	4.1196	0.2096	-	2.9166	0.4804	0.1450	0.0368
GuD(2)	70.8220	17.0419	-	6.3241	1.0715	0.2213	0.0002

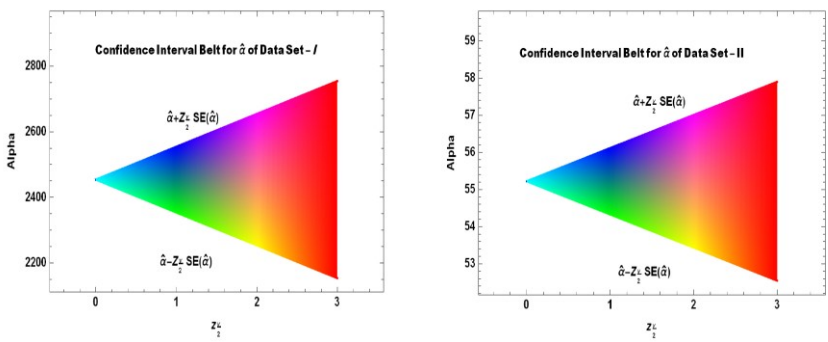

Figure 13
Confidence Interval Belt of $\hat{\boldsymbol{\alpha}}$ for Data Set-I and-II

On the other hand, the well-known loss-of-information criteria, such as Akaike's information criterion (AIC), the corrected version (AICC), Bayesian information criterion (BIC), Hannan-Quinn information criterion (HQIC), and consistent AIC (CAIC) are recommended for model selection in cases where traditional goodness-of-fit metrics are unable to distinguish the better model due to overlapping results. The applicability of the model is further supported by Tables 4(b) and 5(b), which demonstrate that the proposed model has the least loss of information for both data sets.

7.4 *Hydrological Parameters*

The AMF series is extensively used in FFA for two primary reasons. First, its accessibility, as most data is structured in a way that makes annual series easily available. Second, there is a clear theoretical foundation for extrapolating the frequency of AMF series data beyond the observed range (see Hosking and Wallis [9], Hamed and Rao [7], and Hasan [8]). As a result, classical frequency analyses are conducted on all AMF series. Since the PRD model has been identified as the most appropriate based on the two data analyses mentioned earlier, we now proceed to explore other hydrological characteristics through return period estimation, leveraging the properties of this model.

Table 5(b)

Information criterion for the Data Set-II

Distribution	$-l$	**AIC**	**AICC**	**BIC**	**HQIC**	**CAIC**
PRD	371.019	748.038	748.299	755.731	751.148	758.7311
Kappa(3)	372.448	750.897	751.158	758.59	754.007	761.59
GD(3)	383.824	771.647	771.776	776.776	773.72	778.776
WD(2)	397.187	798.374	798.503	803.503	800.447	805.503
GD(2)	384.589	773.178	773.307	778.306	775.251	780.306
EVD(2)	376.169	756.337	756.466	761.466	758.41	763.466
LLD(2)	383.481	770.962	771.091	776.09	773.035	778.09
LND(2)	381.702	767.404	767.533	772.533	769.477	774.533
GuD(2)	412.409	828.817	828.946	833.946	830.891	835.946

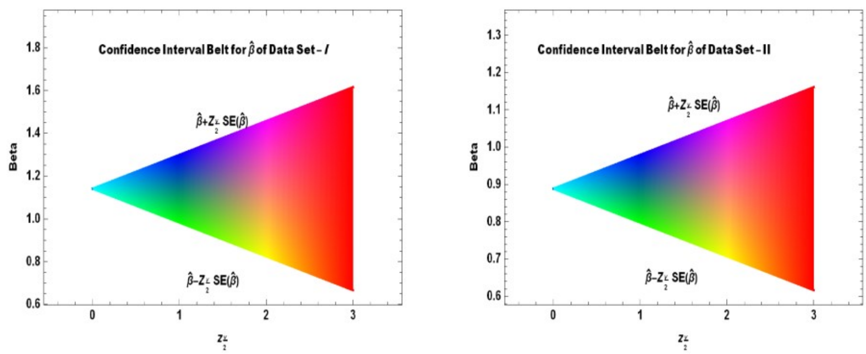

Figure 14

Confidence Interval Belt of $\widehat{\beta}$ for Data Set-I and-II

7.4.1 Return Period

The occurrence of events, such as windstorms, tornadoes, and floods, at least once is often expressed in terms of a return period length, typically denoted by $\mathcal{T}$. This return period is the inverse of the probability that an event will be exceeded in a given year (see Hamed and Rao [7]). The relationship between exceedance probability and the annual return period can now be described in the manner below.

$$\mathcal{F}(x_{\mathcal{T}}) = \mathfrak{P}(X \leq x_{\mathcal{T}}) = 1 - \frac{1}{\mathcal{T}},$$

which implies

$$\mathfrak{p} = \mathfrak{P}(X > x_{\mathcal{T}}) = \frac{1}{\mathcal{T}},$$

hence $\mathcal{T} = \frac{1}{\mathfrak{p}}$, where $\mathcal{F}(x_{\mathcal{T}}) = 1 - (1 - e^{-(\frac{\alpha}{x_{\mathcal{T}}})^{\theta}})^{\beta}$ is probability of non-exceedence and $x_{\mathcal{T}}$ is a high threshold whose probability of exceedance is $\mathfrak{p}$. Therefore, the return level $x_{\mathcal{T}}$ for the PRD can be calculated using the following expression

$$x_{\mathcal{T}} = \alpha\left(-ln\left(1 - \left(\frac{1}{\mathcal{T}}\right)^{\frac{1}{\beta}}\right)\right)^{-1/\theta}, \alpha, \beta, \theta > 0,$$

where $x_{\mathcal{T}} > 0$ and $\mathcal{T} \geq 1$. The Table-6(a) delivers the return level estimates $x_{\mathcal{T}}$ and Table-6(b) yields estimated times of the recurrence of flood, for the data set separately against the return periods $\mathcal{T} = 5, 10, 20, 25, 30, 40, 50$ years and return periods $x_{\mathcal{T}}$ where $\mathcal{T} = \frac{1}{\mathfrak{P}(x_{\mathcal{T}})}$, where $\mathfrak{P}(x_{\mathcal{T}}) = \mathcal{SF}(x_{\mathcal{T}})$ is the SF of the PRD given by

Table 6(a)

Return levels against specific time period ($\mathcal{T}$)

Data Set	5	10	20	25	30	40	50
I	3650.27	4503.14	5498.38	5856.39	6164.31	6680.52	7108.41
II	71.5256	81.0074	91.3619	94.9274	97.9338	102.858	106.838

$$\mathcal{SF}_{\text{PRD}}(x|\alpha, \theta, \beta) = (1 - e^{-(\frac{\alpha}{x})^{\theta}})^{\beta}, x \geq 0, \alpha, \beta, \theta > 0.$$

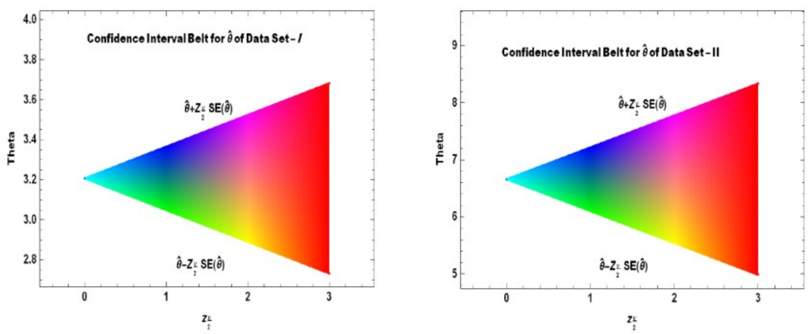

Figure 15

Confidence Interval Belt of $\widehat{\theta}$ for Data Set-I and-II

In computations, the existing parameters are replaced by their estimates $\hat{\alpha}$, $\hat{\theta}$ and $\hat{\beta}$ that indicate the MLEs of the PRD for the comparable data set. Additionally, the plots in Figure 16 for the mentioned data sets suggest that the proposed model represents a realistic (neither excessively long nor too short) return period when compared to the alternative models. Such comparison is also portayed in Table-6(a) and Table-6(b) that clearly indicates that after 50 years the flood discharge will be about 7108.41 cfs and 106.838 m^3/s for data set-I and -II, respectively. Similarly, Figure 16 portrays the the return period which is more realistic when compared with other competing models. Other competing models portray higher time periods for occurrence of such floods, which affects the feasibility of construction and administritations of reservior.

Table 6(b)

Return period against some thershold values (x_T)

Data Set	5000	5500	6000	7000	8000	9000	10000
I	14.3389	20.0208	27.2477	47.3094	76.6052	117.423	172.25
Data Set	45	50	60	80	100	120	140
II	1.01817	1.14824	2.08517	9.31755	33.9225	99.2331	246.766

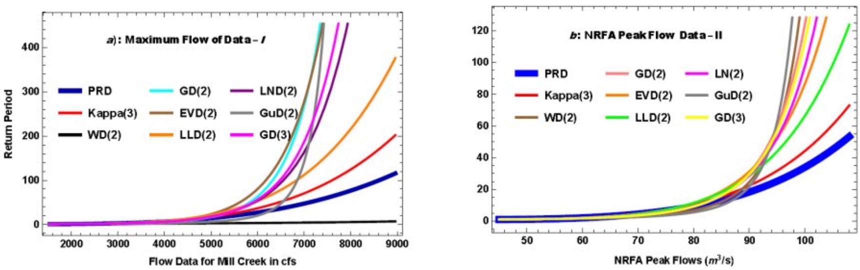

Figure 16

Competing Models' Return Periods for the Data Set-I and -II

8. Conclusion

This article introduces and analyzes a flexible probability model, the power reciprocal distribution. We examine its key mathematical and statistical properties, including the mode, hazard function, asymptotic distributions, quantiles, Mellin and Laplace transformations, as well as order statistics and their asymptotic forms. To assess the validity of the estimated parameters, we characterized the model using the hazard function and Mellin transformation, and estimated its parameters through L-moments and likelihood methods. We also evaluated the model's accuracy by applying it to two real-world flood data sets. The results showed that the proposed model offers greater reliability, assisting engineers in designing reservoirs for practical timeframes. In this context, various flood data assumptions were calculated and validated, including checks for independence, trend, stationarity, outlier detection, and the autocorrelation function (ACF). Additionally, we have outlined plans for future studies, which will focus on determining confidence intervals using various estimation techniques, such as Bayesian methodology and joint probability modeling.

References

[1] D. B. Boorman, A review of the Flood Studies Report rainfall-runoff model parameter estimation equations, Institute of Hydrology, IH Report No. 94, unpublished (1985).

[2] E. Bommier, Peaks-Over-Threshold Modelling of Environmental Data, Uppsala University Department of Mathematics (U.U.D.M.), Project Report 2014:33 (2014).

[3] C. Cunnane, Statistical distributions for flood frequency analysis, Operational Hydrology Report No. 33, WMO No. 718, World Meteorological Organization, Geneva, Switzerland (1989).

[4] J. Deng, "Maximum entropy method for flood frequency analysis: A case study of the Grand River in Ontario, Canada," in IOP Conference Series: Earth and Environmental Science, vol. 344, no. 1, pp. 012002, IOP Publishing (Oct. 2019).

[5] J. F. England, Jr., T. A. Cohn, B. A. Faber, J. R. Stedinger, W. O. Thomas, Jr., A. G. Veilleux, J. E. Kiang, and R. R. Mason, Jr., Guidelines for determining flood flow frequency-Bulletin 17C (ver. 1.1, May 2019), U.S. Geological Survey Techniques and Methods, book 4, chap. B5, pp. 148 (2018). [Online]. Available: https://doi.org/10.3133/tm4B5

[6] I. S. Gradshteyn and I. M. Ryzhik, Table of Integrals, Series, and Products, 7th ed. Academic Press (2007).

[7] K. Hamed and A. R. Rao, Flood Frequency Analysis. CRC Press (2019).

[8] I. F. Hasan, "Flood frequency analysis of annual maximum streamflows at selected rivers in Iraq," *Jordan Journal of Civil Engineering*, vol. 14, no. 4, pp. 573 (2020).

[9] J. R. M. Hosking and J. R. Wallis, Regional Frequency Analysis: An Approach Based on L-Moments. Cambridge, United Kingdom: Cambridge University Press (1997).

[10] V. Kumar, K. V. Sharma, T. Caloiero, D. J. Mehta, and K. Singh, "Comprehensive overview of flood modeling approaches: A review of recent advances," *Hydrology*, vol. 10, no. 7, pp. 141 (2023), https://doi.org/10.3390/hydrology10070141.

[11] A. Khadim, A. Saghir, T. Hussain, and M. Shakil, "Some new developments and review on T-X family of distributions," *Journal of Statistics Applications & Probability*, vol. 11, no. 3, pp. 739-757 (2022), http://dx.doi.org/10.18576/jsap/110301

[12] M. R. Leadbetter, G. Lindgren, and H. Rootzen, Extremes and Related Properties of Random Sequences and Processes. New York: Springer-Verlag (1987).

[13] N. Millington, S. Das, and S. P. Simonovic, "The comparison of GEV, Log-Pearson Type 3 and Gumbel distributions in the Upper Thames River Watershed under global climate models," Water Resources Research Report No. 81, Facility for Intelligent Decision Support, Department of Civil and Environmental Engineering, London, pp. 81 (2011).

[14] R. H. McCuen, Modeling Hydrologic Change: Statistical Methods. CRC Press (2016).

[15] H. Neufeldt, L. Christiansen, and T. W. Dale, Adaptation Gap Report 2020. Nairobi, Kenya: United Nations Environment Programme (2021).

[16] M. H. Nouri Gheidari, "Comparisons of the L- and LH-moments in the selection of the best distribution for regional flood frequency analysis in Lake Urmia Basin," *Civil Engineering and Environmental Systems*, vol. 30, no. 1, pp. 72-84 (2013).

[17] P. M. Rowinski, W. G. Strupczewski, and V. P. Singh, "A note on the applicability of log-Gumbel and log-logistic probability distributions in hydrological analyses: I. Known pdf," *Hydrological Sciences Journal*, vol. 47, no. 1, pp. 107-122 (2002).

[18] V. K. Rohatgi and A. M. E. Saleh, An Introduction to Probability and Statistics. John Wiley & Sons (2015).

[19] M. Sagrillo, R. R. Guerra, and F. M. Bayer, "Modified Kumaraswamy distributions for double bounded hydro-environmental data," *Journal of Hydrology*, vol. 603, pp. 127021 (2021).

[20] A. Smith, C. Sampson, and P. Bates, "Regional flood frequency analysis at the global scale," *Water Resources Research*, vol. 51, pp. 539-553 (2015), https://doi.org/10.1002/2014WR015814.

[21] SAS Institute Inc., SAS/STAT 14.2 User's Guide. Cary, NC, USA: SAS Institute Inc. (2016).

[22] Z. Ur Rehman, C. Tao, H. S. Bakouch, R. Izem, M. O. Kaya, and N. Khan, "A Flexible Bounded Distribution: Information Measures and Lifetime Data Analysis," *Bulletin of the Malaysian Mathematical Sciences Society*, vol. 46, no. 3, pp. 115 (2023), https://doi.org/10.1007/s40840-023-01507-0.

[23] V. L. Webster and J. R. Stedinger, "Log-Pearson Type 3 Distribution and Its Application in Flood Frequency Analysis. I: Distribution Characteristics," *Journal of Hydrologic Engineering*, vol. 12, no. 5, pp. 482-491 (2007), https://doi.org/10.1061/(ASCE)1084-0699(2007)12:5(482).

[24] Z. A. Zakaria, J. M. A. Suleiman, and M. Mohamad, "Rainfall frequency analysis using LH-moments approach: A case of Kemaman Station, Malaysia," *International Journal of Engineering and Technology*, vol. 7, no. 2, pp. 107-110 (2018).

Received April, 2025